Analysis of Uncomplexed and Copper-complexed Methanobactin with UV/Visible Spectrophotometry, Mass Spectrometry and NMR Spectrometry

Lee Behling, Alan DiSpirito, Scott Hartsel, Larry Masterson, Gianluigi Veglia and Warren Gallagher

The titration of methanobactin with Cu(II) was monitored by both UV/Vis and NMR spectroscopy and indicates that the major transitions occurring when Cu(II) interacts with methanobactin involve a two-step process that is complete by about 0.6 Cu:mb. This suggests that a 2:1 complex is formed between methanobactin and copper at low copper levels. If this complex exists, it would be different than the 1:1 complex whose structure was solved for in the crystal state. Also, mass spectral data obtained at low copper levels has revealed only 1:1 complexes of methanobactin and copper. NMR and mass spectrometry reveal that some lots of methanobactin contain a second species of methanobactin that is missing its C-terminal methionine residue. Both these species bind Cu(II) and can be readily separated from one another in the copper-complexed state using HPLC. However, attempts to separated the two species in an uncomplexed state leads to extensive degradation of the methanbactin. Evidences suggests that may be due to the presence of dilute acetic acid in the HPLC solvents. Nearly all of the ^{1}H resonances in methanobactin have been assigned and these have produced a couple of surprises. In the copper-complexed state, the amide proton for Tyr5 shows no coupling to its Hα proton. Also, the assignments indicate that the N-terminus in not capped by an isopropyl ester to the THI1 residue, but, more likely is an isobutyl ester. However, the mass spectral data contradicts this conclusion. The Tyr5 H_N also produces some other contradictory results, some which suggest a restricted environment when in the the copper-complexed state, and others suggesting a more mobile environment. Up to 90% of the copper can be removed from copper-complexed methanobactin by dialysis against Na_2EDTA. NMR spectroscopy shows a structure for the EDTA treated methanobactin that is very similar to that for the copper-complexed methanobactin, indicating that the structural transitions that occur upon copper binding are irreversible.

A. Introduction

Methanobactin (mb) is a 9 residue peptide that is produced by methanotophic bacteria. Fro methanobactin that is isolated from *Methylosinus trichosporium* OB3b, 7 of the residues are standard amino acids: Gly2-Ser3-Cys4-Tyr5 and Ser7-Cys7-Met9; while the remaining two are novel imidazole and thiocarbonyl containing residues: *N*-2-isopropylester-(4-thiocarbonyl-5-hydroxyimidazole) (THI1) and pyrrolidine-(4-hydroxy-5-thiocarbonylimidazole) (HTI6).

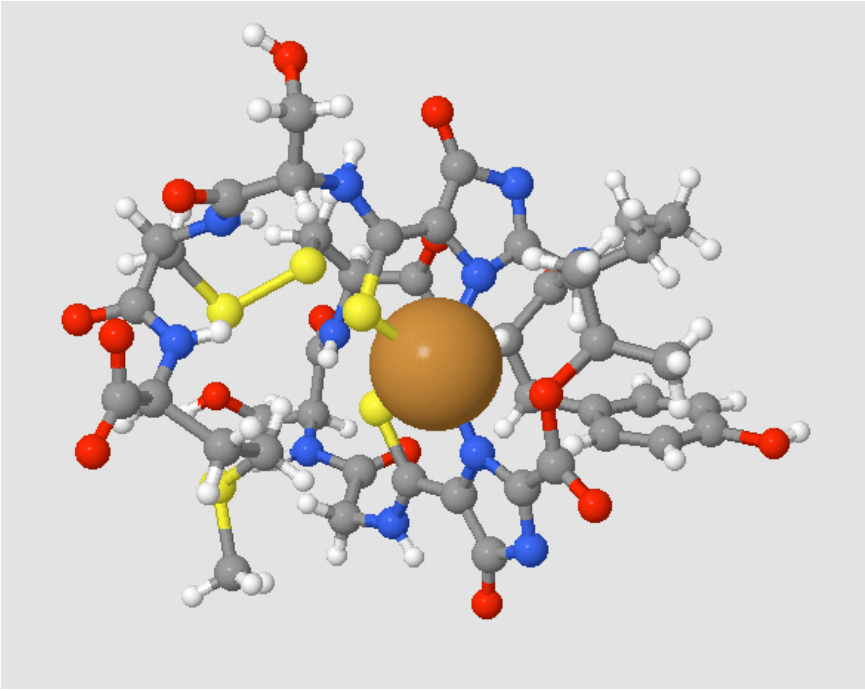

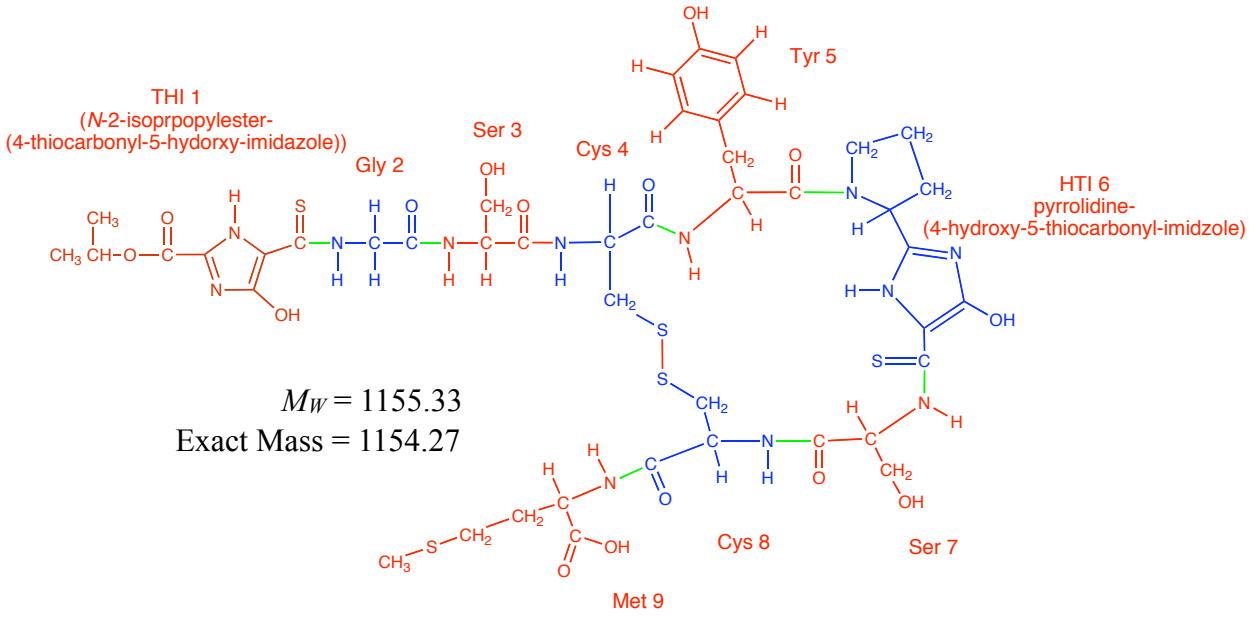

M_W = 1155.33
Exact Mass = 1154.27

A crystal structure for a copper-complexed form of methanobactin has been reported by Kim *et al.*, 2004.[1] The crystal structure was obtained with crystals that were grown at a 1000 to 1 excess of Cu(II) to methanobactin[2] and shows a 1 to 1 complex of copper and mb. In the crystal structure the copper ligated to the two thiocarbonyl sulfur atoms coming from each of the imidazole containing residues (THI and HTI), along with one nitrogen from each of the two imidazole groups. The copper-complex state of methanobactin is known to be considerably more stable than the uncomplexed state.[3] Recently, DiSprito *et al.* reported a procedure for obtaining purified methanobactin in an uncomplexed state.[3] This has opened the door to studying the the process by which methanobactin binds and reduces Cu(II) to Cu(I). A series of studies using UV/Vis spectrophotometry, XPS, EPR and fluorescence spectroscopy have been carried out to look

at the interactions of Cu(II) with methanobactin at low Cu(II) to mb ratios.[2] Here we report results obtained using NMR and mass spectroscopy.

B. Observations

Monitoring the titration of uncomplexed methanobactin with Cu(II) with UV/Vis spectrophotometry.

Before presenting the results that were obtained for monitoring the titration of methanobactin with Cu(II), we will first look at the results of extending the analysis of the UV/Vis data to demonstrate that the early portion of the the titration is dominated by a two-step process. The top panel in Figure 1 shows an overlay of 21 spectra collected during a titration of methanobactin with copper(II) sulfate. The copper to methanobactin ratio during this titration ranged from 0.0 to 2.0 Cu:mb. The predominant peaks at 340 nm and 394 nm have been assigned to the HTI and THI residues, respectively.[2] Other potential chromophores include the cysteine/cystine groups and the phenolic side chain of Tyr 5. The middle and bottom panels of Figure 1 show the first two principle components from a singular value decomposition of the spectra shown in the top panel. This was done after subtracting the average spectrum from each of the 21 spectra. The first component is the only one with a singular value greater than 1 (2.4), and accounts for 66% of the observed variations in the UV/Vis spectra that occur from 0.0 Cu:mb to 2.0 Cu:mb. Together, the first two components account for approximately 80% of the observed variations.

The spectra were also analyzed using the two-dimensional correlation analysis that was developed by Noda *et al*. for the analyzing changes in infrared spectra.[4] Figure 2 shows a two-dimensional contour plot of the synchronous changes that occur during the titration. Plots of the overlaid spectra are shown to the top and right of the two-dimensional plot, for reference. The correlation spectrum is dominated by changes that occur synchronously with changes occurring at 394 nm. By carrying out similar analyses on subsets of the 21 spectra data set (not shown), it can be demonstrated that the synchronous process shown in Figure 2 is complete by 0.6 Cu:mb. The plot of the first principle component from Figure 1 has been overlaid along a line at 394 nm to show that these synchronous changes are well accounted for by the first principle component. Since only a single component is needed to account for these changes it can be argued that the changes are the result of a single two-state process. This conclusion is corroborated by the numerous isosbestic points that are observed in the overlaid spectra (Figure 1, top panel).

Figure 3 shows the corresponding asynchronous component of the two-dimensional correlation analysis. The plot of the second principle component from Figure 1 has been overlaid along a line at 394 nm to show that the changes that occur asynchronously with the changes that occur at 394 nm are well accounted for by the second principle component. Bt looking at subsets of the 21 spectra, it can be shown that the asynchronous process, which accounts for 14% of the total observed changes, involves primarily changes at 394 nm and 254 nm. The asynchronous changes extend out to 2.0 Cu:mb.

Monitoring the titration of uncomplexed methanobactin with Cu(II) with NMR.

The Cu(II) titration of a uniformly ^{15}N-labeled sample of methanobactin (Lot N) was monitored by NMR spectroscopy. The sample was dissolved at 2 mM concentration in 9 mM phosphate buffer, *pH*6.5, containing 10% D_2O. ^{15}N-HSQC spectra were collected at 600 MHz at 25°C. The titration was carried out by adding aliquots of a 100 mM $CuSO_4$ solution to the methanobactin solution. Up to a 0.2 unit drop in the *pH* was observed after each addition. The *pH* was readjusted to *pH*6.5 after each addition using 100 mM KOH. The ^{15}N-HSQC spectra collected at selected points in the titration are shown in Figure 4. Starting at 0.0 Cu:mb, there is a set of 7 peaks in the amide region of the spectrum, which diminish in intensity as the Cu(II) is added, and are gone by 0.4 to 0.6 Cu:mb. Concomitantly, there is a second group of 11 peaks that grow in to replace the original 7, with the transition appearing to be complete by 0.6 Cu:mb. This concerted transition from one set of peaks to a second set of peaks supports a two-state transition on the NMR timescale and agrees with what is observed when the titration was monitored with UV/Vis spectrophotometry.

Figure 5a shows a plot of the peak volumes for the resonances that appear in the ^{15}N-HSQC spectra during the Cu(II) titration *versus* the Cu:mb ratio. It illustrates how one set of peaks disappears as a new set grows in. The transition appears to be complete by 0.6 Cu:mb. Figure 5b shows Figure 5D from Choi *et al.*, 2006,[2] which plots changes at selected wavelengths in the UV/Vis spectra of mb during a titration with Cu(II), and illustrates that the behavior that we are seeing with NMR spectroscopy mirrors that which has been published by others. Choi *et al.*, 2005[3] have reported that EPR spectroscopy shows that for Cu:mb ratios up to 0.4 Cu:mb, all of the added Cu(II) binds to mb and is reduced to Cu(I). Together, theses results suggest that methanobactin is forming a 2 to 1 complex with Cu(II) and, concomitantly, reducing the Cu(II) to Cu(I). This would make this complex different than the one observed in the crystal structure reported by Kim *et al.*, 2004,[1] which shows a 1 to 1 complex of copper to methanobactin.

It should be kept in mind that the interpretation of the titration data critically depends on an accurate measurements of the methanobactin concentration. Choi *et al*., 2006[2] report a set of extinction coefficients for both the uncomplexed and copper bound methanobactin, which we have used for most of our experiments. The concentration of the methanobactin used in for the Cu(II) titration that was monitored by ^{15}N-HSQC (Figure 4), however, used a mass-based concentration. We usually find that the mass concentration usually gives a lower estimate of the methanobactin concentration, by about 10 to 20%, when compared to the UV/Vis absorption based concentration. Figure 6 shows the UV/Vis absorbances at selected wavelengths *versus* Cu:mb for the same data set that was used in Figures 1, 2 and 3. A lower estimate of the methanobactin was used to bias the Cu:mb to higher values. Except for the absorbance at 254 nm, the effects brought about by the addition of Cu(II) appear to level off well before 1.0 Cu:mb and stay that way up to 2.0 Cu:mb.

Figures 7a and 7b show the ^{15}N-HSQC spectra obtained at the starting and ending points of the titration that was monitored by ^{15}N-HSQC and compares them to the corresponding 1–dimensional ^{1}H spectra. They focus on the amide and aromatic region of the proton spectra.

Figure 7c shows an overlay of the two for comparison. The H_N peaks show less broadening after the mb interacts with the Cu(II) and a greater of number peaks appear than disappear during the titration. Methanobactin contains 7 amino acid residues, each which participates in either an amide or thioamide bond. There are also 5 additional nitrogen atoms, which could potentially be protonated; two in each of the two imidazolate groups, and one in the pyrrolidine ring portion of the HTI residue. The pyrrolidine ring is connected to Tyr5 by an amide bond, and like proline, is not expected to be protonated at neutral *pH* values. For the copper-complex form there are a pair of N-H singlets that appear around 7 ppm, suggesting a protonation of one or both of the imidazolate groups of residues (THI1 and HTI6).The apparent lack of *J*-coupling for each of the these peaks suggests that they are each part of an isolated spin system. The ^{1}H-TOCSY spectra of the Cu-complexed mb appears to corroborates this (Figure 8), however, there is other NMR evidence, which is presented later, that will show that theses two peaks arise from the Tyr 5 H_N in two different species of methanobactin. There are also some peaks that appear to reduced or missing in the ^{15}N-HSQC spectra, in particular, the Ser3 and Ser7 residues.

Figures 7a, 7b and 8 show the ^{1}H assignments that we have made for this region of the spectrum. The rationale used to make these assignments will be described later. At first, the double set of resonances that are observed for the all of the amino acid residues except Gly 2 and Met 9 upon binding copper was attributed to multiple conformations for the methanobactin upon binding copper. This interpretation seemed plausible given the apparent 2 to 1 ratio for the methanobactin-copper complex. This interpretation was abandoned, however, when we looked at third lot of methanobactin. The ^{15}N-labeled methanobactin that was used to collect the ^{15}N-HSQC spectra we are calling Lot N, and the lot of methanobactin that was used to collect the ^{1}H spectra shown in Figures 7 and 8 we are calling Lot B. It turns out that both of these lots contain two different species of methanobactin. This became evident to us when we started collecting ^{1}H spectra on methanobactin from a third lot, which we are calling Lot A. The ^{1}H spectrum, along with the ^{1}H-TOCSY spectrum for methanobactin Lot A, are shown in Figure 9. There appears to be very little of the second species in this lot. Later we will show that this second species is missing its C-terminal methionine residue, Met9. In Comparing Figures 7a, 7b and 8, it appears that both are able to bind copper, but produce different structures in the copper-complex state.

Figure 10 compares the ^{1}H spectra for the Lot A of methanobactin in both the uncomplexed and copper-complex states. It illustrates the changes in the chemical shifts that occur upon binding and reducing Cu(II). The resonances for the aromatic protons shows the doublet of doublets in both states, indicating that the tyrosine side chain freely rotates on the NMR time scale in both states. They do, however go from weakly coupled spin system to a more strongly coupled spin system. There is also evidence that the the Hδ resonance in Cu-complexed methanobactin moves upfield of the Hε resonance, compared to its downfield location for the uncomplexed methanobactin.

Fractionation of Uncomplexed Methanobactin

The preliminary NMR results that were carried out on the different lots of methanobactin indicate the presence of more than one species in some of the lots. There is also considerable lumpiness to the baseline in the ^{1}H NMR spectra. Consequently, an effort was undertaken to try and separate and clean up the two species.

First, an ESI-TOF mass spectrum was run on the Lot A sample in negative ion mode (Figure 11a). It show a predominant species with a *m/z* of 576.14. The 1/2 amu spacing in its isotope pattern (see Figure 11a inset), indicates it carries a -2 charge. This value agrees with the calculated value of 576.13 for uncomplexed methanobactin $(M\text{-}2H^{+})^{2-}$, which contains a disulfide bond. The structure shown above has a disulfide bond between the two cysteine side chains, as is observed in the crystal structure for the copper-complexed methanobactin. However, other possible disulfide bonds, which involve the thiocarbonyl sulfurs, can be envisioned. The C-terminal carboxyl group is the obvious choice as the source for one of the -1 charges. Possible sources for the other include the phenolic hydroxyl group of the tyrosine side chain, the imidazolate hydroxyl group of either the THI or HTI residue, or, after an enol to enthiol tautomeric shift, the thiol group of either the THI or HTI residue.

An ESI-TOF mass spectrum was also run on the Lot B sample in negative ion mode (Figure 11b). In addition to the $(M\text{-}2H^{+})^{2-}$ species that was seen in the mass spectrum for Lot A, there is also a M^{-2} ion peak at 510.62 and a M^{-1} ion peak at 372.10. The 510.62 species has m/z value that agrees with the 510.61 value expected for the -2 ion state of uncomplexed methanobactin that is missing its C-terminal Met9 residue $(M\text{-}M9\text{-}2H^{+})^{2-}$. A possible identity for the 372.10 species will be discussed later.

Attempts were made to fractionate and further purify the uncomplexed form of both Lot A and Lot B methanobactin using HPLC. Initially runs were carried out on an LC/MS using an Agilent C_{18} reverse phase column (Agilent Eclipse XDB-C18, 4.6 mm x 150 mm, 5µm bead size) and monitoring with an ESI-TOF mass spectrometer detector (Agilent 6210). The samples were eluted with an H_2O/MeOH gradient containing 0.1% acetic acid. Little or no material corresponding to the uncomplexed methanobactin was observed eluting from the LC, however, small amounts of the copper-complexed form were observed. Copper-complexed methanobactin does represent a trace contaminant in the uncomplexed methanobactin samples (see Figure 11a inset).

We then tried doing the HPLC using a semipreparative reverse phase column (Hamilton PRP-3, 7.0 mm x 305 mm, 10µm bead size, 300Å pore size) and monitoring with a diode-arrray detector (Varian ProStar 330). The samples were eluted with an H_2O/MeOH gradient containing 0.001% acetic acid. The top panel in Figure 12 show the elution profile obtained when a sample of methanobactin Lot A was loaded on this column and eluted with a 1% to 99% linear MeOH gradient and monitored at 340 nm. Figure 12 shows that three peaks are observed. The third peak, Fraction 3, is the most prominent peak and has a UV/Vis spectrum that is characteristic of the uncomplexed methanobactin (see the bottom panel of Figure 12), with peaks at approximate

394 nm, 340 nm and 300 nm, and a broad shoulder extending through 280 nm to 250 nm. The fraction that comes off immediately before Fraction 3 has a spectrum that is similar to Fraction 3, but has a 340 nm peak that is reduced relative to the others. This peak was tentatively assigned to the HTI6 residue by Choi *et al*., 2006,[2] with the 394 nm peak assigned to the THI1 residue. The selective loss of absorbance by the 340 nm peak suggests that, alternatively, this may actually be the THI1 residue, which as the N-terminal residue and could be lost while leaving the other chromophores intact. Fraction 1 shows two peaks, one at 329 nm and another at 257 nm. If the 340 nm peak in methanobactin spectrum arises from the N-terminal THI1 residue, this may represent an N-terminal degradation product of methanobactin. Further isolation and characterization of these fractions should allow us to resolve these questions.

Figure 13 shows the results of a similar HPLC run performed on a sample of methanobactin Lot B. The elution profile shown in the top panel of this figure shows that Lot B produces a greater number of fractions than Lot A. The most prominent one, which goes off scale in the figure and is labeled Fraction 5, appears to correspond to Fraction 3 for the Lot A profile. It has a UV/Vis spectrum that is characteristic of methanobactin. Fraction 3 from the Lot B run has a UV/Vis spectrum that is almost identical to that for Fraction 5, suggesting it too contains a nearly intact form of methanobactin. Fraction 4 also has a methanobactin-like spectrum, but with a reduced 340 nm absorbance, similar to Fraction 2 from the Lot A run. Fraction 2 has a very interesting spectrum, which appears to complement the one for Fraction 1 from the Lot A profile. Like that fraction, it has two major peaks in its spectrum, but instead they are located at 389 nm and 296 nm. If the 340 nm peak in the methanobactin does represent the THI1 residue, as suggested above, then the 394 nm absorbance would arise from the HTI6 residue. If the 389 nm peak in the Fraction 3 spectrum is due to HTI6, then the 296 nm peak in this fraction could coming from the adjacent tyrosine residue, Tyr5. Fraction 1 appears to contain a mixture of what is found in Fraction 2 from the Lot B run and Fraction 1 from the Lot A run. Both the Lot A and Lot B HPLC runs indicate that a considerable amount of degradation in the uncomplexed methanobactin has taken place, much more than anticipated from the mass spectra for these lots (see Figure 11).

In an effort to further identify the various degradation products the fractions from the Lot B HPLC run (Figure 13) was subjected to ESI-TOF mass spectroscopy. The results are shown in Figure 14. Both Fraction 1 and 2 contain -1 species with m/z values of 372.07 and 394.07 in different proportions. In the last paragraph we suggested that Fraction 2 may contain a fragment that contains the Tyr5-HTI6 residues. If the hydrolysis of this fragment from full length methanobactin produced a thiocarboxylate C-terminal, its -1 fragment would have a m/z of 375.11:

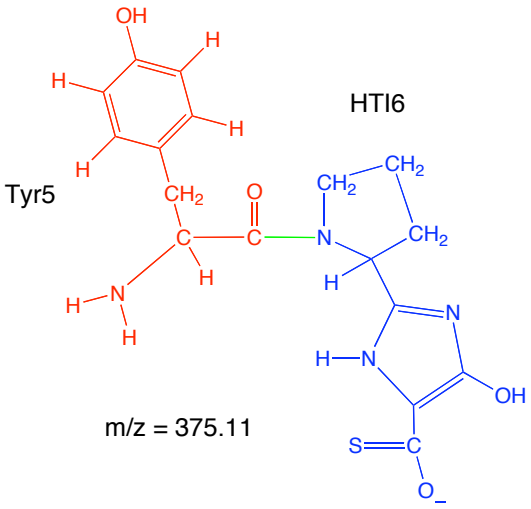

The 3 amu difference in the m/z value from 372.07 is significant. The production of the thiocarboxylate from the degradation is questionable, since the sulfur is expected to be a better leaving group than the nitrogen during a hydrolysis reaction. If Fraction 1 from the Lot A run contains the N-terminus THI1, as described above, then the inclusion of the next two residues will produce -1 species with an m/z close to 372.10:

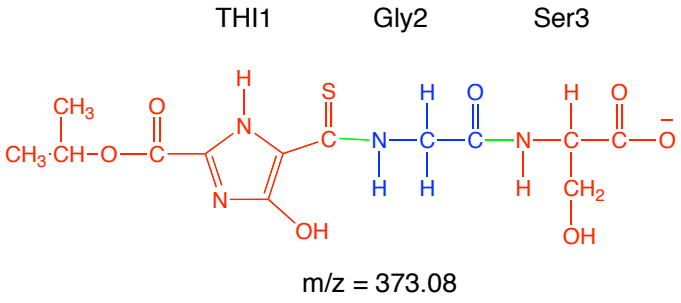

Again close, but a 1 amu difference is still considered significant.

The mass spectrum for Fraction 5 shows that this fraction contains the undegraded methanobactin; the m/z value of 576.13 agrees exactly with the expected value for the $(M\text{-}2H^{+})^{2-}$ species of methanobactin, The 1153.25 m/z value agrees with the calculated value of 1153.27 for the $(M\text{-}H^{+})^{1-}$ species of methanobactin. For Fraction 3, which has a UV/Vis spectrum that is nearly identical to that for Fraction 5, the predominant species has a m/z of 510.61. This value agrees exactly with the expected value for the -2 charged form a methanobactin that is missing its C-terminal Met9 residue, $(M\text{-}M9\text{-}2H^{+})^{2-}$. In summary, The material in Fractions 3 and 5 contain the two species that we expected to observed based on the mass spectrum of the unfractionated Lot B material (see Figure 11b), while the other fractions contain a considerable amount of degraded material.

The material found in Fraction 3 from the Lot A run, and Fraction 5 from the Lot B run, were characterized further by NMR. These were the fractions that contained what appears to be the undegraded methanobactin. The fractions from multiple HPLC runs for each were pooled.

The methanol was pulled from the sample by rotavaporation and the concentrated sample lyophilized. The lyophilize material was dissolved in 9 mM phosphate, *pH*6.5, 10% D_2O and analyzed by NMR spectroscopy. Figure 15 shows the results of these analyses. Figure 15a (the upper spectrum) shows an ^1H spectrum for the unfractionated Lot A for comparison; this is the same spectrum that was shown in Figure 10 (bottom). Figure 15b shows the ^1H spectrum for the Lot A Fraction 3 sample. It shows a marked increase in the number of resonances in the "purified" material. Figure 15b shows the ^1H spectrum for the Lot B Fraction 5 sample along with a ^1H-TOCSY spectrum. Again, it shows a marked increase in the number of resonances. These results suggests that the material in these two fractions continued to degrade after they were eluted form the column and during the concentration process. The ^1H spectra for both Lot A, Fraction 3, and Lot B, Fraction 5 appear similar, suggesting a similar mixture of degradation products were produced by both. The ^1H-TOCSY spectrum for Lot B, Fraction 5 shows multiple H_N chemical shifts for the same spin systems, suggesting they arise from the same residue in multiple degradation fragments (compare Figure 15c with Figure 8).

The conclusion reached from these attempts to fractionate and further purify the uncomplexed methanobactin is that uncomplexed methanobactin is unstable under the conditions used in our procedures. Others have observed that uncomplexed methanobactin is sensitive to light,[5] so we made efforts to minimize the exposure to light during the fractionation. The methanobactin we used was obtained from the spent media of the methanotrophs *Methylosinus trichosporium* OB3b and isolated by elution from a polystyrene-based sorbent resin (Diaion HP-20) with 60% methanol.[3] Therefore, exposure to methanol is not expected to present a problem. The remaining suspect is the acetic acid. We were able to see considerably more undegraded methanobactin coming off of the HPLC column when the eluting solvent contained 0.001% acetic acid instead of 0.1% acetic acid. We also observed the UV spectra noticeably changing from the leading to the lagging side of the peaks as they eluted from the column. This suggests that the uncomplexed methanobactin is degrading during the isolation and that the culprit is the acetic acid. Others too have observed poor resolution when carrying out reverse phase HPLC on methanobactin under acidic conditions.[5] Our results point to degradation of the methanobactin as being cause of this poor resolution. To follow up on this, we are currently looking into carrying out the HPLC runs at neutral and basic *pH* values. We are also interested in isolating and characterizing the degradation products further in order to make more definitive assignments of the absorption bands in the UV/Vis spectrum and to possibly piece together the events occurring during the degradation.

Fractionation of Copper-complexed Methanobactin

Our attempts to further purify the copper-complexed methanobactin have proven more successful. It has been shown that methanobactin that is isolated under condition of high copper concentrations (~1000 fold excess over methanobactin) is quite stable.[5] We have carried out HPCL on copper-complexed methanobactin using the same procedure described above for the uncomplexed methanobactin. We have done this for both Lots A and B. Before loading a methanobactin sample on the HPLC column, it was first titrated with Cu(II)sulfate in 0.1 Cu:mb

intervals, with the *pH* adjusted back to 6.5 after each addition of the the $CuSO_4$. Figure 16 shows the elution profile for a sample of methanobactin Lot B that was made up at 6.1 mM in 10 mM phosphate, *pH*6.5 and titrated to 0.7 Cu:mb with 100 mM $CuSO_4$. The sample was eluted from a Hamilton PRP-3 (7.0 mm x 305 mm, 10µm bead size, 300Å pore size) column with a 1% to 99% methanol gradient containing 0.001% acetic acid. When monitored at 340 nm, the elution profile shows 2 major peaks with a minor peak that lags the second major peak as a shoulder. The UV/ Vis spectra for the major peaks, labeled Fractions 1 and 2, are characteristic of that for methanobactin (see Figure 16), the the spectra for the minor trailing fraction, Fraction 3, appears, on the other hand, to have a reduced absorbance in the 340 nm region. Similar results are obtained when the copper-complexed form of methanobactin A is run, but with Fraction 1 being much reduced compared to Fraction 2 (data not shown).

Figure 17b and 17c show the ESI-TOF mass spectra for Fractions 1 and 2, respectively, for the HPLC run carried out on methanobactin Lot B (see Figure 16). Figure 17a shows the mass spectrum for the unfractionated sample that was loaded on the column. It indicates that there are two primary components in the sample, one with a M^{1-} m/z value of 1215.09 and the other with a M^{1-} value of 1084.06. The corresponding M^{2-} species are also present with m/z values of 607.04 and 541.53, respectively. All of these have the "picket fence" isotope pattern that is characteristic of a copper-complexed species. Copper has two stable isotopes in natural abundance; ^{63}Cu (69%) and ^{65}Cu(31%). The 1215.09 species has a m/z value that agrees well with the 1215.15 value expected for -1 state of a 1:1 complex of Cu(I) with methanobactin, $(M - 2H^+ + {}^{63}Cu)^{1-}$. The 1084.06 species has a m/z that agrees well with the 1084.15 value expected for -1 state of a 1:1 complex of Cu(I) complexed methanobactin that is missing is C-terminal Met9 residue, $(M - M9 - 2H^+ + {}^{63}Cu)^{1-}$. Kim *et al.*, 2005[5] have observed a similar species using MALDI-TOF after intentionally removing the C-terminal amino acid from methanobactin with Proteinase K. Figures 17b and 17c demonstrate that we can use HPLC to separate these two species from one another. They also show that the methionine sulfur atom, which is a good Cu(I) ligand, is not required for copper binding by methanobactin. Missing also are the numerous multiple degradation products that were produced when the same HPLC procedure was applied to the unfractionated methanobactin.

The mass spectrometry results also raise some questions about the stoichiometry of the copper-complexed methanobactin that forms at lower concentrations of Cu(II). The copper to methanobactin ratio that was used for the experiment shown in Figure 17 was 0.7 Cu:mb, yet all of the species observed by mass spectroscopy, both before and after the fractionation by HPLC, contain 1 Cu(I) per methanobactin. Earlier we proposed that methanobactin forms a 2 to 1 methanobactin to copper complex at low copper concentrations. The mass spectrum shows no evidence for such a species, which is expected to have a m/z value of 2369.46 for the $(2M - 2H + {}^{63}Cu)^{1-}$ species, 1184.23 for the $(2M - 3H + {}^{63}Cu)^{2-}$ species, and 790.06 for the $(2M - 43H + {}^{63}Cu)^{3-}$ species. A possible explanation is that the dimer complex dissociates in the electrospray process to produce a 1:1 complex of copper and methanobactin. However, in this case we might expect to see a population of the the uncomplexed methanobactin; and that is not observed either.

Another possible explanation is that we are overestimating our methanobactin concentrations by about two-fold and therefore are working at higher Cu:mb ratios than we think.

The methanobactin Lot B fractions that were analyzed by ESI-TOF mass spectroscopy (see Figure 17) were also analyzed by NMR spectroscopy. The material in Fractions 1 and 2 were concentrated by rotavaporation followed by lyophilization and dissolved in 9 mM phosphate, *pH*6.5, 10% D_2O for the NMR analyses. Figure 18 shows the ^1H spectra in the amide and aromatic region for Fractions 1 and 2 and compare them to that for an unfractionated Lot B sample. The results demonstrate that the multiple resonances that are observed for many of the residues in the Lot B sample are due to the the presence of two different species of methanobactin that are present in this Lot; the spectra for the two fractions combine nicely to produce the spectrum observed for the unfractionated sample. There are some additional resonances in the spectrum of the Fraction 2, which are marked with stars. These are due to an identified contaminant that was picked during rotavaporation:

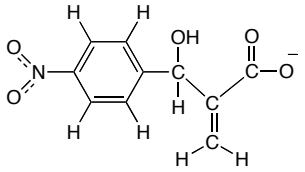

Both the mass spectroscopy data and the NMR data indicate that, unlike the uncomplexed methanobactin, the copper-complexed methanobactin is stable against degradation.

Figure 19 compares the ^1H spectrum for the Lot B Fraction 2 sample with the unfractionated Lot A sample, demonstrating that these two samples are essentially identical. The mass spectrometry data shown in Figures 11a and 17c indicate these samples both contain the undegraded methanobactin. In addition to separating the two species of methanobactin that are found in the Lot B sample of methanobactin, the HPLC fractionation of Lot B appears to have removed some of the lumpiness that is observed in the baseline of he ^1H spectrum for methanobactin Lot A.

Above we described that the material found in Fraction 1 of Lot B has a mass that agrees with that for a methanobactin that is missing its C-terminal Met9 residue. Further NMR analysis of this fraction confirms this. Figure 20a shows the ^1H-TOCSY spectrum in the aliphatic region for the methanobactin Lot B, Fraction 2 and has the Hα, Hβ, Hγ spin system for Met9 mapped out on it. Figure 20b shows the corresponding spectrum for the methanobactin Lot B, Fraction 1. The Hα, Hβ, Hγ spin system for Met9 is totally missing from this spectrum while the other aliphatic resonances from the Fraction 2 spectrum remain. This corroborates the mass spectroscopy data supporting the identity of the second species in Lot B as a methanobactin that is missing its C-terminal methionine residue.

Proton assignments for methanobactin

The ^{1}H assignments were made from a combination of COSY, TOCSY and ROESY spectra. We carried out NOESY and ROESY experiments at both 600 MHz and 400 MHz and at both 5°C and 25°C and found that the 400 MHz ROESY experiment at 25°C gave us the most complete set of NOE's. The NMR experiments were carried out on methanobactin Lot A samples, which were titrated to a copper to methanobactin ratio of 0.5 Cu:mb. As was described above, this lot of methanobactin contains primarily the undegraded methanobactin.

Figure 21a shows the assignments for a 600 MHz TOCSY spectrum in the amide and aromatic region that was collected on a 6 mM sample of methanobactin Lot A in 9 mM phosphate, *pH*6.5, 10% D_2O, 5°C, which was titrated to 0.5 mM Cu:mb. The spin systems for six out of the seven amino acid residues are AMX; the exception is the Met9, which contains an AM(PT)X spin system because of its extra methylene group, making it distinguishable from the others. After identifying the Met9 spin system we were then able to identify those for Gly2, Ser3, Cys4, Ser7 and Cys8 based on the *d(i,i+1)* NOE's that were observed in the 400 MHz ^{1}H-ROESY spectrum (see Figure 22a and 22b). A list of the observed *d(i,i+1)* NOE's are listed Table 1.

No cross peaks for the Tyr5 H_N are observed in either the ^{1}H-COSY or ^{1}H-TOCSY spectra (see Figure 21a). Assignments for the Tyr5 Hα and Hβ protons were made based on the observed NOE's for these protons to the Tyr5 Hδ protons on the phenolic ring (see Figure 22a). TOCSY cross peaks are observed, however, for both the Tyr5 Hα and Hβ protons in the aliphatic region of the ^{1}H-TOCSY spectrum (see Figure 21b).

There is an H_N proton at around 7 ppm, for the copper-complexed mb, which appears as an isolated spin system (see Figure 21a). This resonance also shows up in the ^{15}N-HSQC spectra (see Figure 7b). Initially we believed that this proton was attached to one of the imidazolate ring nitrogens of either the THI1 or HTI6 residue. However, this proton produces a number of NOE's that suggest that it is the Tyr5 H_N (see Figure 22a). The ^{1}H-TOCSY spectrum of an uncomplexed methanobactin Lot A sample (see Figure 23) does show a spin system arising from the Tyr5 H_N with assignments for the Tyr Hα and Tyr Hβ that agree with those obtained from the ROESY spectrum of the copper-complexed Lot A (see Figure 22a). We have consequently assigned the apparent singlet at 7 ppm to the Tyr5 H_N proton, despite of its apparent lack of coupling to the Tyr5 Hα proton after the copper is bound. At this point we have not explanation for why this occurs, except for the possibility that the dihedral angle between the vincinal H_N and Hα protons is ±90°. The observed NOE's for the Tyr5 H_N are listed in Table 1, and include ones to Tyr5 Hα, Tyr5 Hβ, Cys4 Hα, and Ser3 Hα.

The assignments for the 7 protons on the pyrrolidine ring in the HTI residue were made based on the similarity of their spin system to that of a proline residue. These protons are labeled H9, H10, H11, and H12:

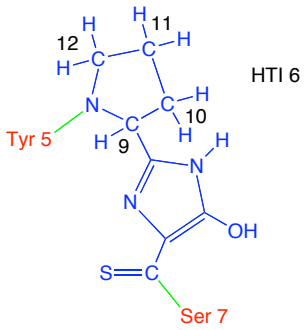

The pyrrolidine ring protons H12 and H9 also show NOE's with the Hδ protons of the Tyr5 side chain. In the crystal structure of methanobactin these two ring systems are packed against one another, so the interaction is not surprising.

The protons in methanobactin that still remain unassigned are those for the isopropyl group, which is part of the THI1 residue and caps the N-terminus of methanobactin:

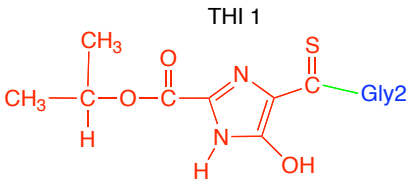

The boxes shown in Figure 21b map out the spin system for this group. The methyl groups produce two doublet resonances at 0.73 and 0.81 ppm. Their doublet splitting is consistent with being attached to a methine carbon. The resonance for the methine group is at 2.1 ppm, which is a ways upfield from what is expected for a methine attached to a carboxylate group as an ester. For example, the chemical shift for the methine proton in isopropyl acetate is around 5 ppm. Another issue that is inconsistent with an isopropyl group is the additional group of protons in this spin system at 3.1 ppm. The spin system appears to more closely resemble that for an isobutyl ester rather than an isopropyl ester. This assignment is supported by the multiplicity-edited ^{1}H-^{13}C-HSQC spectrum, which was run on a copper-complexed methanobactin Lot A sample (see Figure 24). In this plot, crosspeaks for carbons with 1 or 3 hydrogens attached are negatively phased (red), while those with 2 hydrogens attached are positively phased (blue). However, the mass spectroscopy data on copper-complexed methanobactin do not support the additional methylene carbon that would be required for an isobutyl group; if this is an isobutyl ester, then another 14 amu needs to be removed from elsewhere on the structure. We do not yet have an explanation for this mystery. Kim *et al.*, 2005[6] report selectively hydrolyzing the ester and determining the mass of what is left by MALD-TOF mass spectroscopy. There results are consistent with an isopropyl ester. Interestingly, in comparing the ^{1}H spectra for methanobactin with the methanobactin that is missing its C-terminal Met9, the proposed isobutyl methylene resonance at 3.1 ppm (compare Figures 20a to Figure 20b) collapses from an ABX type type triplet splitting to an AA'X doublet with the loss of the methionine from the other end of the molecule. This suggests a possible interaction between the N and C termini of the intact methanobactin.

Assessing the mobility and solvent accessibility of the amide protons

Measuring the temperature dependence of the the chemical shifts for the amide protons in a peptide can be used to assess the hydrogen bonding environment of peptide amides, especially if this is done in conjunction with measuring the hydrogen/deuterium isotope exchange rate for same protons.[6] As the temperature increases the donor-acceptor distance will tend to increase as a results of thermal motion, leading to an upfield shift in the chemical shift for the proton participating in the hydrogen bond. For folded protein and peptides structures that are stable over the temperature range examined, the effect is typically greater for amides that are hydrogen bonded to solvent molecules than to those that are involved in intermolecular hydrogen bonding. How this might be applied to methanobactin is questionable. The inability so far to obtain long-range NOE's suggests that the structures that we are dealing with, even for the copper-bound state of methanobactin, may be quite dynamic. Also, the crystal structure for methanobactin shows that none of the peptide amide nitrogens appear to be participating as donors in intermolecular hydrogen bonding. Nonetheless, the temperature dependence for the the chemical shifts for the amide protons does show a range values for copper-complexed methanobactin. Figure 24a shows a plots of the chemical shift for the seven amide peptides *versus* temperature of a 6 mM methanobactin Lot A sample that was dissolved in 9 mM phosphate, *pH*6.5, 10% D_2O. The temperature ranged from 5°C to 23°C. Figure 24b shows a bar chart of the slopes ($\Delta\delta/\Delta T$) in units of ppb/K. The general interpretation for these analyses is that $\Delta\delta/\Delta T$ values more negative than -4.5 ppb/K are an indication of hydrogen bonding to solvent, especially if the amide undergoes rapid hydrogen isotope exchange. On the otherhand, values less negative than this are an indication of intermolecular hydrogen bonding, especially if the amide is more slowly exchanging. Figure 24b indicates that the Ser3 amide proton has the most negative $\Delta\delta/\Delta T$ value at -7.2 ppb/K. This is not surprising since the Gly2 and Ser3 amide proton resonances are usually quite broad and often display solvent exchange peaks in the TOCSY and ROESY spectra, indicating considerable mobility and rapid proton exchange with the solvent.

The next most negative $\Delta\delta/\Delta T$ value is that for the Tyr 5 amide proton at -4.8 ppb/K. This one is a bit more surprising, given its location in what is probably the most rigid region of the molecule. If the two cysteine side chains form a disulfide bond, as they do in the crystal structure, then the backbone portion of the Tyr5 residue, along with those of the Cys4, HTI6, Ser7 and Cys8, are members of a 20 atom ring, which should greatly reduce the mobility of the atoms in the ring. With the exception of the Tyr5 amide proton, the amide protons for the other members of this ring display small negative $\Delta\delta/\Delta T$ values (see Figure 25), with the adjacent Cys4 amide proton having the lowest value. In the crystal structure the, Cys4-Tyr5-HTI6 segment appears to be the most constrained part of the molecule. They form a tight β-like turn with the Tyr5 involved in a *cis*-peptide bond to the nitrogen in the pyrrolidine ring of the HTI6 residue. The large number of NOE's that involve Tyr5 (see Table 1), also support a reduced mobility for this portion of the molecule.

The $^3J_{HN\text{-}H\alpha}$ coupling constants are shown in Figure 24c. Again, the Cys4 and Tyr5 residues distinguish themselves with the largest and smallest values, respectively. The $^3J_{HN\text{-}H\alpha}$ coupling

constant for Cys4 is 10.0 Hz, while for the Tyr5 the splitting is unobservable; the H_N resonance appearing as a singlet with a linewidth of approximately 4.5 Hz. As discussed earlier, The H_N resonance for the Tyr5 shows no coupling to its Hα resonance in the COSY and TOCSY spectra of methanobactin when in its copper-bound state. Table 2 lists the backbone dihedral angles that are observed in the crystal structure of methanobactin[1] along with the corresponding $^3J_{HN\text{-}H\alpha}$ coupling constants. The high value for the Cys4 ^3J value is in line with the φ dihedral angle of approximately 120°. Based on the values for the φ dihedral angles in the crystal structure, the $^3J_{HN\text{-}H\alpha}$ coupling constants for Ser3, Ser7 and Met9 should be the smallest, while that for the Tyr5, at around -65° should be comparable to that for Cys8. The fact that we are not observing this may indicate that we are looking at a different structure than the one observed in the crystal state.

We also carried out a hydrogen/deuterium isotope exchange experiment on copper-complex methanobactin to see if any of the amide protons were protected from exchange. A sample of methanobactin Lot A that was dissolved in 9 mM phosphate, *pH*6.5, 10% D_2O was lyophilized; and then redissolved in 100% D_2O. It was placed immediately in NMR spectrometer and ^1H spectra were taken a regular time intervals. Figure 25 shows the results of this experiment for four of the intervals. The dead time for the experiment was 177 s. By that time all of the amide protons had exchanged for deuterons, except Cys4 and Tyr5. The Cys4 was gone by 236 s, while the Tyr5 appears to linger the longest, lasting until 339 s. These results appear to support the other finding that indicate that this appears the be the most static region of the methanobactin molecules, however, it seems to also contradict the conclusion of the the Δδ/ΔT experiment.

Comparing the structure of copper-complexed methanobactin with EDTA treated methanobactin.

Choi *et al*, 20062 have shown that up to 90% of the copper that is complexed with methanobactin, which was isolated in the presence of high Cu(II) concentrations, can be removed by dialysis against Na_2EDTA. Based on UV/Vis and circular dichroism data they proposed that the structure of the EDTA treated methanobactin after exposure to Cu(II) is similar to that of the copper-complexed methanobactin. They also showed that the EDTA treated methanobactin can rebind Cu(I). We obtained a sample of EDTA treated methanobactin, which we analyzed with NMR and mass spectroscopy. Figure 27 shows the ^1H spectrum in the amide region of the EDTA treated methanobactin and compares it to copper-complexed methanobactin Lot A. The EDTA treated methanobactin shows a bit more lumpiness to its baseline, but otherwise is quite similar to the copper-complexed methanobactin Lot A. There is one additional peak in the EDTA treated methanobactin's spectrum at around 7.95 ppm. In the ^1H-TOCSY spectrum of this sample (not shown) this resonance produces a cross peak with the Tyr5 Hα proton, suggesting that there may be a second alternative environment for the Tyr5 residue in the EDTA treated methanobactin.

We have also looked at the EDTA treated methanobactin with ESI-TOF mass spectroscopy. Figure 28 shows the results of this analysis. We see a major species with an m/z of 607.10, which corresponds to the M^{2-} ion of the 1:1 complex of copper and methanobactin $(M - 3H + {}^{63}Cu)^{2-}$.

There are no apparent species that correspond to uncomplexed methanobactin; most of the other minor species in the spectrum appear to be bound to copper. This is surprising given the EDTA treatment was suppose to remove 90% of the copper. The situation is similar to one discussed earlier, where only the 1:1 copper-complexed state of methanobactin is observed when uncomplexed methanobactin is exposed to sub-equivalent amounts of Cu(II) (see Figure 17). Either the uncomplexed methanobactin is no longer present in these samples, or, it is incapable of forming ions by electrospray ionization.

[1] Kim, H. J., Graham, D. W., DiSpirito, A. A., Alterman, M. A., Galeva, N., Larive, C. K., Asunskis, D., and Sherwood, P. M. (2004) Methanobactin, a copper-acquisition compound from methane-oxidizing bacteria, *Science 305*, 1612-1615.

[2] Choi, D. W., Zea, C. J., Do, Y. S., Semrau, J. D., Antholine, W. E., Hargrove, M. S., Pohl, N. L., Boyd, E. S., Geesey, G. G., Hartsel, S. C., Shafe, P. H., McEllistrem, M. T., Kisting, C. J., Campbell, D., Rao, V., de la Mora, A. M., and Dispirito, A. A. (2006) Spectral, kinetic, and thermodynamic properties of Cu(I) and Cu(II) binding by methanobactin from Methylosinus trichosporium OB3b, *Biochemistry 45*, 1442-1453.

[3] Choi, D. W., Antholine, W. E., Do, Y. S., Semrau, J. D., Kisting, C. J., Kunz, R. C., Campbell, D., Rao, V., Hartsel, S. C., and DiSpirito, A. A. (2005) Effect of methanobactin on the activity and electron paramagnetic resonance spectra of the membrane-associated methane monooxygenase in Methylococcus capsulatus Bath, *Microbiology (Reading, England) 151*, 3417-3426.

[4] Noda, I. (1990) 2-Dimensional Infrared (2d Ir) Spectroscopy - Theory and Applications, *Appl Spectrosc 44*, 550-561.

[5] Kim, H. J., Galeva, N., Larive, C. K., Alterman, M., and Graham, D. W. (2005) Purification and physical-chemical properties of methanobactin: a chalkophore from Methylosinus trichosporium OB3b, *Biochemistry 44*, 5140-5148.

[6] Baxter, N. J., and Williamson, M. P. (1997) Temperature dependence of 1H chemical shifts in proteins, *Journal of biomolecular NMR 9*, 359-369.